Journal of
Plankton Research

plankt.oxfordjournals.org

J. Plankton Res. (2015) 37(5): 1074–1087. First published online April 22, 2015 doi:10.1093/plankt/fbv024

Contribution to the ICES/PICES Theme Session: 'Interactions of Gelatinous Zooplankton within Marine Food Webs'

Population drivers of a *Thalia democratica* swarm: insights from population modelling

NATASHA HENSCHKE[1,2,3]*, JAMES A. SMITH[1,2], JASON D. EVERETT[1,2] AND IAIN M. SUTHERS[1,2]

[1]EVOLUTION AND ECOLOGY RESEARCH CENTRE, UNIVERSITY OF NEW SOUTH WALES, SYDNEY NSW 2052, AUSTRALIA, [2]SYDNEY INSTITUTE OF MARINE SCIENCE, BUILDING 22, CHOWDER BAY ROAD, MOSMAN NSW 2088, AUSTRALIA AND [3]SCHOOL OF BIOLOGICAL, EARTH AND ENVIRONMENTAL SCIENCES, UNIVERSITY OF NEW SOUTH WALES, SYDNEY, NSW 2052, AUSTRALIA

*CORRESPONDING AUTHOR: n.henschke@unsw.edu.au.

Received September 4, 2014; accepted March 19, 2015

Corresponding editor: Marja Koski

The small salp, *Thalia democratica*, is known globally to form dense swarms, yet the physiological and oceanographic factors that influence the magnitude and occurrence of these swarms are poorly understood. In this study, two numerical models were used to explore *T. democratica* population dynamics. A Lefkovitch matrix model identified that the survival of juvenile oozoids was the most important population metric promoting population growth and a size-structured population model was developed to further explore the dynamics of *T. democratica*. The size-structured model tracks cohorts of four life stages and incorporates size-dependent reproduction and mortality. Model outputs of average generation time and mean abundances of each life stage corresponded well to previously reported values. Factors that promote juvenile oozoid abundance were the most sensitive parameters influencing salp abundance. A 10-year time-series simulation using this population model identified that salp abundances in the Tasman Sea are proportionally higher in winter and spring, consistent with previous studies. This model shows that temperature and phytoplankton concentration are sufficient drivers of large-scale patterns of salp abundance across season and latitude. These results demonstrate the importance of future research focusing on identifying the environmental conditions that influence the size at which females reproduce.

KEYWORDS: *Thalia democratica*; salp population model; salp swarm; zooplankton; size-structured; Tasman Sea

INTRODUCTION

Pelagic tunicates such as salps have a major role in marine ecosystems. They often form large swarms after the upwelling of cool, nutrient rich water promoting blooms of phytoplankton (Henschke *et al.*, 2011). Salps feed more efficiently on phytoplankton than other zooplankton (Harbison and Gilmer, 1976; Blackburn, 1979),

consuming particles from <1 μm to 1 mm in size (Vargas and Madin, 2004; Sutherland *et al.*, 2010). They rapidly transfer this energy out of the euphotic zone through fast-sinking carbon-rich faecal pellets (Bruland and Silver, 1981) and carcasses (Henschke *et al.*, 2013; Lebrato *et al.*, 2013). When salps occur in large swarms (up to 5003 ind. m^{-3}; Everett *et al.*, 2011), the carbon flux from salp faecal pellets can be 10-fold greater than the average daily flux (Fischer *et al.*, 1988), revealing the large input salp swarms can make to the biogeochemical cycle (Henschke *et al.*, 2013).

Despite the ecological importance of salps, there is a lack of data on basic ecological traits such as growth and mortality rates, primarily due to the difficulty in culturing salps in the laboratory (Heron, 1972; Harbison *et al.*, 1986; Raskoff *et al.*, 2003). There is also little information on the temporal evolution of salp swarms or how demographic characteristics or population growth rates change with time and oceanographic conditions. Experimental studies have shown that both temperature and chlorophyll *a* (chl-*a*) drive variability in growth rates (Heron, 1972; Deibel, 1982; Henschke *et al.*, 2014); however, the structure of these relationships and the conditions that provide "optimal" growth rates are unknown. The occurrence of swarms of some salp species is strongly seasonal with the peak abundance occurring in spring (Heron, 1972; Licandro *et al.*, 2006; Henschke *et al.*, 2014), which suggests that the optimal temperature and chl-*a* conditions driving growth rates occur at this time.

Salp populations are characterized by alternating generations of sexually reproducing blastozooid and asexually reproducing oozoid life history stages (Fig. 1; Heron, 1972). Population-level traits such as the blastozooid-to-oozoid ratio and generation time may drive salp abundance (Henschke *et al.*, 2014). The blastozooid-to-oozoid ratio has been used in several studies as a tool to determine what stage of swarm formation the salp population is in (Menard *et al.*, 1994; Loeb and Santora, 2012). Generation time is calculated as the time taken from birth of a female blastozooid to birth of the next generation of female blastozooids, and is positively correlated with growth rates (Heron, 1972). Observational sampling of these life history characteristics often only provides a snapshot of swarm demographics. By exploring the temporal resolution of a salp swarm using a numerical model that can be assessed against observed data, one can identify how these traits may vary during the creation of a swarm under different environmental conditions. For example, the blastozooid-to-oozoid ratio or generation time of a seed population may determine the success of future swarm development.

The ubiquitous small salp, *Thalia democratica*, is the most abundant salp in the Tasman Sea (Thompson and Kesteven, 1942; Henschke *et al.*, 2011). Swarms of *T. democratica* are regularly observed in the Tasman Sea (Deibel and Paffenhofer, 2009; Baird *et al.*, 2011; Everett *et al.*, 2011; Henschke *et al.*, 2011), but there are no continuous long-term zooplankton time-series along the south-east Australian coast (Hobday *et al.*, 2006; Poloczanska *et al.*, 2007) which track the development and decline of salp swarms. The most recent spatially comprehensive salp survey for the Tasman Sea was done 50 years ago (Tranter, 1962), with smaller scale sampling occurring from 2002 (Henschke *et al.*, 2011, 2014). One way to enhance our understanding of salp population dynamics is through numerical modelling.

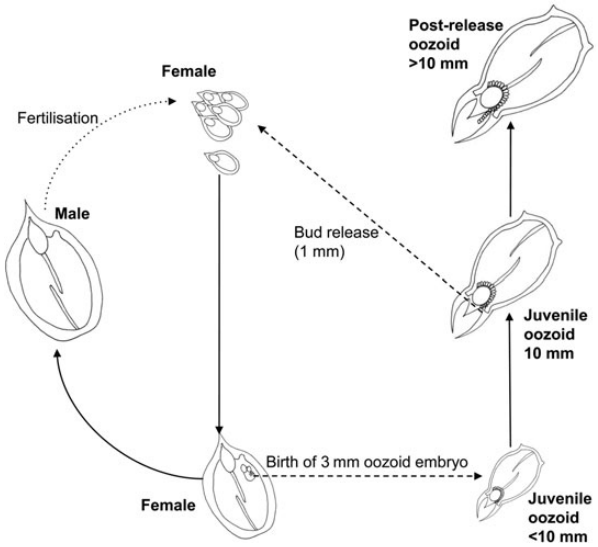

Fig. 1. Life cycle of *Thalia democratica* showing four life history stages used in the models: females, males, juvenile oozoids and post-release oozoids. See Table I for life history information. Modified from Fig. 1 in Henschke *et al.* (Henschke *et al.*, 2011).

In this study, two numerical models were used to explore the population dynamics of *T. democratica*. A Lefkovitch (Lefkovitch, 1965) matrix model was used to identify the life history stage which has the greatest influence on population size. A size-structured population model was developed to describe changes in *T. democratica* abundance in response to environmental conditions. This included simulations using observed sea surface temperature (SST) and chl-*a* data from three sites on the south-east Australian coast. Specifically, the aims of this study were to develop and implement a numerical model in order to: (i) identify the most influential life history stage in the generation of salp swarms; (ii) explore how the distribution, abundance and life history traits of salp swarms change under different oceanographic conditions; and (iii) identify which model parameters most strongly influence model outputs.

Table I: Life history stages of Thalia democratica *included in the models and shown in Fig. 1*

Generation	Life history stage	Size (mm)	Stage duration (days)	Daily survivorship	Lifetime fecundity
Blastozooid	Female	>1	4.92	0.84	1
Blastozooid	Male	>4	16.79	0.55	0
Oozoid	Juvenile oozoid	3–10	5.5	0.89	0
Oozoid	Post-release oozoid	>10	14.29	0.55	60.5

Table II: Four-stage population matrix for the salp Thalia democratica

0.7939	0	0	4.233
0.1994	0.55	0	0
0.2034	0	0.8162	0
0	0	0.1791	0.7458

METHOD

General approach

Two models were used to examine the temporal dynamics within a *T. democratica* population. A Lefkovitch (Lefkovitch, 1965) stage class matrix model was used to identify which life stage of *T. democratica* has the greatest influence on population growth. Then, a size-structured population model was developed which incorporated both temperature and phytoplankton dependent growth. Temperature and phytoplankton abundance (chl-*a* concentration) were used as the external drivers in this model, given their known association with salp abundance (Licandro *et al.*, 2006; Deibel and Paffenhofer, 2009). Only these two environmental variables were used as long-term analyses have found both temperature (25 years; Licandro *et al.*, 2006) and phytoplankton abundance (17 years; Stone and Steinberg, 2014) to be the most significant environmental drivers of *T. democratica* abundances. In both models, *T. democratica* had four life history stages (Fig. 1; Table I): (i) females, which was the blastozooid life stage from birth (female buds) until release of a juvenile oozoid; (ii) males, which was the life stage formed from females that have released a juvenile oozoid; (iii) juvenile oozoids, which was the life stage of an oozoid until the release of female buds (at around 10 mm length); and (iv) post-release oozoids, which was the life stage of oozoids after the release of female buds.

Lefkovitch matrix model

The Lefkovitch matrix (Lefkovitch, 1965) is a stage-structured model of population growth, and is used to forecast future population states. It assumes that the population will either grow or decline linearly, and that each stage class will grow at the same rate. In a constant environment, the proportion of individuals in each stage class of a population tends toward a steady-state (stable-age) distribution (Lotka, 1925). As a result, the Lefkovitch matrix can be used to identify critical life history transitions. The Lefkovitch matrix for *T. democratica* takes the form of a population projection matrix:

$$\begin{array}{c} \begin{matrix} \text{F} & \text{M} & \text{J} & \text{PR} \end{matrix} \\ \begin{bmatrix} P_1 & 0 & 0 & F_4 \\ G_1 & P_2 & 0 & 0 \\ F_1 & 0 & P_3 & 0 \\ 0 & 0 & G_3 & P_4 \end{bmatrix} \end{array} \quad \begin{matrix} \text{Females (F)} \\ \text{Males (M)} \\ \text{Juvenile oozoids (J)} \\ \text{Post - release oozoids (PR)} \end{matrix}$$

where F_i is the stage-specific fecundity, P_i is the probability of surviving and remaining in the same stage and G_i is the probability of surviving and growing to the next ith stage (also known as the transition probability). P_i and G_i are calculated based on stage duration and survivorship (Table I) and presented with F_i in Table II. Fecundity (Table I), survival [Equation (7)] and growth estimates [Equation (15)] are based on published data presented in the size-structured population model below.

The dominant eigenvalue (λ) of the Lefkovitch matrix is used to calculate population growth

$$N_t = N_{t-1}\lambda \qquad (1)$$

where N is the number of total individuals at time t. When $\lambda = 1$, the population remains constant in size through time. When $\lambda < 1$, the population declines geometrically, and when $\lambda > 1$, the population increases geometrically.

Sensitivity analysis reveals how very small changes in both F_i and P_i will affect λ when the other elements in the matrix are held constant. This is calculated using the stable stage distribution (w; right eigenvector) and stage-specific reproductive values (v; left eigenvector). The elasticity matrix shows the sensitivity of population growth (λ) to changes in survival within the same stage. Because the elasticities of these matrix elements sum to 1, they can be compared directly in terms of their contribution with the population growth rate. For more information on how sensitivity analyses are conducted for Lefkovitch matrix models, see Caswell (Caswell, 1989).

Size-structured population model

The size-structured population model is a discrete-time model, following cohorts of each life history stage, at an hourly time step. It is size-structured because it uses size-dependent reproduction and mortality, where growth is dependent on food consumption (phytoplankton carbon concentration) and temperature (Fig. 2). Temperature and phytoplankton carbon concentration values are derived from a 10-year time-series (2003–2012) of satellite calculated SST and chl-*a* values. Phytoplankton carbon was calculated from the available chl-*a* using a chl-*a*-to-phytoplankton carbon ratio (CPR) of 1:90.6977 (Mullin, 1983). Phytoplankton carbon was used instead of chl-*a* mass to correspond to mass-specific clearance rates (Deibel, 1985). This relationship is explained in further detail below [Equation (16)].

Salp abundance

The abundance of salps at time t is given by:

$$\mathcal{N}_t = \sum (\mathrm{Nf}_{t,n} + \mathrm{Nm}_{t,n} + \mathrm{Nj}_{t,n} + \mathrm{Np}_{t,n}) \qquad (2)$$

where $\mathcal{N}_t$ is the total salp abundance (ind. m^{-3}), $\mathrm{Nf}_{t,n}$ is the abundance of females, $\mathrm{Nm}_{t,n}$ is the abundance of males, $\mathrm{Nj}_{t,n}$ is the abundance of juvenile oozoids and $\mathrm{Np}_{t,n}$ is the abundance of post-release oozoids from the nth generation at time t.

The abundance of females is calculated:

$$\mathrm{Nf}_{t+1,n} = \mathrm{Nf}_{t,n} \times \mathrm{e}^{-\mathrm{Mf}_t} - (\mathrm{Nf}_{t,n} \times \mathrm{Rf}_t) + (\mathrm{Rs}_t \times \mathrm{Nj10}_{t,n-1}) \qquad (3)$$

where Mf_t is the instantaneous female mortality rate (h^{-1}), Rf_t is the actual female reproduction rate (oozoids female^{-1} h^{-1}), Rs_t is the oozoid reproduction rate (female buds oozoid^{-1} h^{-1}) and $\mathrm{Nj10}_{t,n-1}$ is the abundance of juvenile oozoids (ind. m^{-3}) that are 10 mm long from the $n-1$ generation at time t. The term $\mathrm{Nf}_{t,n} \times \mathrm{Rf}_t$ represents the females that have recently reproduced and transitioned into males, and the term $\mathrm{Rs}_t \times \mathrm{Nj10}_{t,n-1}$ represents the female buds that were recently released from a juvenile oozoid.

The abundance of males is calculated:

$$\mathrm{Nm}_{t+1,n} = (\mathrm{Nm}_{t,n} \times \mathrm{Mm}) + (\mathrm{Nf}_{t,n} \times \mathrm{Rf}_t) \qquad (4)$$

where Mm is the male mortality rate (h^{-1}).

The abundance of juvenile oozoids is calculated:

$$\mathrm{Nj}_{t+1,n} = \mathrm{Nj}_{t,n} \times e^{-\mathrm{Mj}_t} + (\mathrm{Nf}_{t,n} \times \mathrm{Rf}_t) - \mathrm{Nj10}_{t,n} \qquad (5)$$

where Mj_t is the juvenile oozoid mortality rate (h^{-1}). $\mathrm{Nf}_{t,n} \times \mathrm{Rf}_t$ also refers to the abundance of juvenile oozoids born at time t as each female can only produce one offspring.

When juvenile oozoid length is >10 mm (at $\mathrm{Nj10}_{t,n}$; Heron, 1972), juvenile oozoids give birth to females and transition into post-release oozoids. Therefore within the

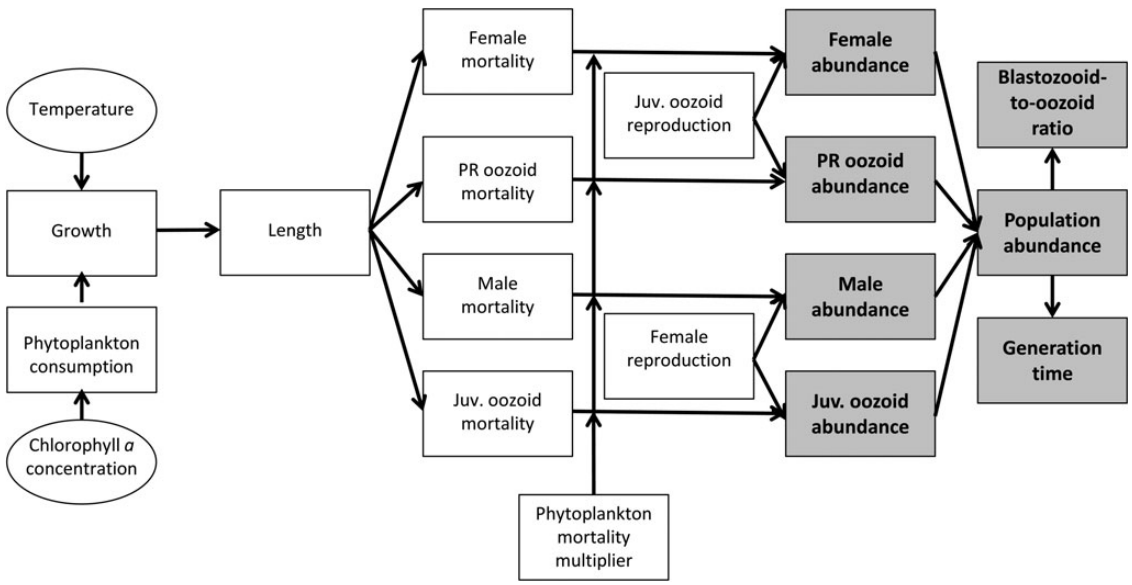

Fig. 2. Model schematic showing interactions between the forcing functions (white ovals), model variables (white boxes) and the model outputs (grey boxes).

Table III: Parameter values used in the model simulation

Parameters	Equation	Description	Value	Units	Source
a	7	Female mortality coefficient	0.025	h^{-1}	Inferred from Deibel (Deibel, 1982)
b	7	Female mortality exponent	1.06	h^{-1}	Inferred from Deibel (Deibel, 1982)
c	7	Juv. oozoid mortality coefficient	0.038	h^{-1}	Inferred from Deibel (Deibel, 1982)
d	7	Juv. oozoid mortality exponent	1.06	h^{-1}	Inferred from Deibel (Deibel, 1982)
mm	8	Male mortality rate	0.03	h^{-1}	Andersen and Nival (Andersen and Nival, 1986)
mp	8	Post-release oozoid mortality rate	0.02	h^{-1}	Best guess[a]
K	10, 11	Phytoplankton carrying capacity	3.26/2.15/3.34	mg C m^{-3}	Maximum from 10-year time-series for Coffs Harbour, Sydney and Eden
T_{opt}	14	Optimal temperature	17	°C	Inferred from Licandro *et al.* (Licandro *et al.*, 2006)
σ_T	14	Temperature standard deviation	2.5	°C	Inferred from Thompson (Thompson, 1948)
h	15	Maximum growth coefficient	1.491	mm mm^{-1} h^{-1}	Heron (Heron, 1972)
j	15	Maximum growth exponent	0.313	mm^{-1}	Heron (Heron, 1972)
CR	16	Mean hourly carbon requirement	2	% body C	Deibel (Deibel, 1985)
o	17	Body mass coefficient	0.25	mg C m^{-3} h^{-1}	Deibel (Deibel, 1985)
p	17	Body mass exponent	2.31	mg C m^{-3} h^{-1}	Deibel (Deibel, 1985)
L_{50}	19	Female length at 50% reproducing	8	mm	Heron (Heron, 1972)
MF_{50}	20	Male:female ratio for 50% reproduction success	0.025	–	Best guess[b]
$\boldsymbol{\mu}_{Rj}$	21	Mean oozoid fecundity	81.78	ind. $sol.^{-1}$	Deibel and Lowen
$\boldsymbol{\sigma}_{Rj}$	21	Oozoid reproduction standard deviation	10	ind. $sol.^{-1}$	Best guess[c]

Parameters used in the sensitivity analysis are in bold. Parameter values were estimated from the cited literature or inferred (see Method section for details).
[a]Inferred from low proportional abundances sampled in the field (Henschke, unpublished data).
[b]Estimated from proportional abundances found in the field (Henschke, unpublished data).
[c]Chosen to give an oozoid fecundity range of 40–120 ind. sol^{-1}.

same generation, the abundance of post-release oozoids is calculated:

$$\mathrm{N}p_{t+1,n} = \mathrm{N}p_{t,n} \times \mathrm{M}p_t + \mathrm{Nj}10_{t,n} \quad (6)$$

where $\mathrm{M}p_t$ is the post-release oozoid mortality rate (h^{-1}). The division between the two oozoid stages was made as a mathematical convenience, to ensure only one release of female buds per oozoid.

Mortality rate

The length-based instantaneous total mortality rate for females and juvenile oozoids is given as negative power curves. The parameter values are based on laboratory experiments (Deibel, 1982) and, in this model, mortality is also dependent on phytoplankton concentration:

$$\mathrm{M}f_t = a(\mathrm{L}f_t)^{-b} \times \mathrm{PM}_t \quad (7)$$

where $\mathrm{M}f_t$ is female mortality rate (h^{-1}), $\mathrm{L}f_t$ is female length (mm) and PM_t is the phytoplankton concentration mortality multiplier at time t [see Equations (9)–(11)]; a and b are constants (Table III). The same equation is used for juvenile oozoid mortality rate ($\mathrm{M}j_t$), where juvenile oozoid length ($\mathrm{L}j_t$) replaces female length ($\mathrm{L}f_t$) and the constants c and d replace a and b.

As males are known to die after fertilization, independent of length (Miller and Cosson, 1997), their mortality rate includes a constant:

$$\mathrm{M}m_t = 1 - \mathrm{mm} \times \mathrm{PM}_t \quad (8)$$

where $\mathrm{M}m_t$ is male mortality rate (h^{-1}) at time t and mm (h^{-1}) is a constant. This constant (mm) was calculated assuming males have the same mortality rate as young females (Andersen and Nival, 1986), and is equal to the average mortality rate for a 1–2 mm female individual. Similarly, oozoids post-release are given a mortality rate ($\mathrm{M}p_t$) irrespective of length where mm is replaced by mp. As oozoids are generally found in much lower abundances than blastozooids (females and males; e.g. Henschke *et al.*, 2014), it is assumed that after birth of females, post-release oozoids will have a mortality rate similar to, but not as high as, males. As there are no data available on stage-specific mortality rates, it is difficult to accurately determine the mortality relationship for older life history stages (males and post-release oozoids). Both males and post-release oozoids have little effect on population abundances due to their low abundances and no reproductive output (Heron, 1972); hence, salp population abundance is likely to be relatively insensitive to variations in their mortality rates. Regardless, the mortality rate parameters are included in our sensitivity analysis.

The phytoplankton concentration mortality multiplier (PM_t) increases salp mortality when phytoplankton concentration is low. This multiplier is necessary to

incorporate mortality due to starvation, as without it the only impact of low phytoplankton concentrations on the salp population are reduced growth rates. Coefficients f and g are parameterized so that mortality is 10 times the normal rate when phytoplankton concentration is equal to 0.09 mg C m^{-3} (0.001 mg chl-*a* m^{-3}). This was calculated based on Threlkeld (Threlkeld, 1976) who states that when zooplankton are starved, mortality will equal 100% after 5 days:

$$\mathrm{PM}_t = f\,(\mathrm{NP}_t - C_t)^g \tag{9}$$

$$f = \frac{1}{K^{\overline{-1\log_{10}(K)+3}}} \tag{10}$$

$$g = \frac{-1}{\log_{10}(K)+3} \tag{11}$$

where NP_t is the concentration of available phytoplankton carbon at time t (mg C m^{-3}), C_t is the total concentration of phytoplankton consumed by salps at time t (mg C m^{-3}) and K is the maximum phytoplankton carbon value expected ("carrying capacity"; mg C m^{-3}). Given that this model uses phytoplankton from a time-series of observed data, it is necessary to reduce the concentration of phytoplankton to that which can be consumed by salps while ensuring a sustainable supply remains. It would be spurious to allow salps to consume all phytoplankton without acknowledging the positive concentration of phytoplankton in the following time step. Thus, the satellite-derived chl-*a* was reduced using a production:biomass (PB) ratio of 0.014 h^{-1} to calculate the concentration of chl-*a* available for salp consumption. PB ratios are commonly used to estimate the biomass that can be sustainably removed from a standing stock biomass (Ney, 1990; Christensen and Pauly, 1992). K was set at the maximum phytoplankton carbon concentration calculated from a 10-year time-series of data from either the Coffs Harbour, Sydney, or Eden coast (2003–2012) depending on the location of the time-series simulation.

Length and growth rate

Female body length is calculated as:

$$\mathrm{Lf}_{t+1} = \mathrm{Lf}_t + (G_t \times \mathrm{Lf}_t) \tag{12}$$

where Lf_t is the length of the female (mm) and G_t is the growth rate (mm mm^{-1} h^{-1}) at time t. The same equation is used to calculate length for each life history stage, with Lf_t replaced by the respective length for each stage.

Growth is proportional to phytoplankton consumption and temperature, and is calculated:

$$G_t = \mathrm{Gmax}_t \times \frac{\mathrm{NP}_t}{C_t} \times \Delta T_t \tag{13}$$

where G_t is the actual temperature and phytoplankton dependent growth rate (mm mm^{-1} h^{-1}), Gmax_t is the maximum length-dependent growth rate (mm mm^{-1} h^{-1}) and ΔT_t is the deviation of the temperature (T_t; °C) at time t from the temperature (T_{opt}; °C) at which Gmax_t occurs (i.e. the optimal temperature). Growth (G_t) equals Gmax_t when salp total consumption (C_t) is less than the available phytoplankton concentration (NP_t); i.e. when food supply exceeds food demand. As C_t begins to exceed NP_t, G_t decreases. There are little data available to validate the structure of this consumption-based growth component, and future models may benefit from investigating the relationship between consumption and growth rate in more detail.

A normal distribution is used to describe the declining growth rate of salps on either side of T_{opt}, and ΔT_t is found using the following normal probability density:

$$\Delta T_t = \frac{f\,(T_t|T_{\mathrm{opt}}, \sigma_T)}{f\,(T_{\mathrm{opt}}|T_{\mathrm{opt}}, \sigma_T)} \tag{14}$$

where σ_T is a parameter used to specify the range of temperatures at which *T. democratica* occurs (Thompson, 1948). This is the same for each stage.

Maximum length-dependent growth rate is the same for each stage is calculated from Heron (Heron, 1972) using an exponential equation:

$$\mathrm{Gmax}_t = he^{-jL_t} \tag{15}$$

where L_t is the stage-specific length (mm) at time t; h and j are constants.

Phytoplankton consumption rate

The salp population's total phytoplankton consumption (C_t; mg C h^{-1}) is equal to the sum of stage-specific consumption and is based on average mass-specific clearance rates calculated for *T. democratica* (Deibel, 1985):

$$C_t = \mathrm{CR} \times (\mathrm{Bf}_t \times \mathrm{Nf}_t + \mathrm{Bm}_t \times \mathrm{Nm}_t + \mathrm{Bj}_t \times \mathrm{Nj}_t + \mathrm{Bp}_t \times \mathrm{Np}_t) \tag{16}$$

where CR is the mean hourly consumption required by a *T. democratica* individual (set at 2% of body mass as carbon), Bf_t is the body mass of females (mg C m^{-3}), Bm_t the body mass of males, Bj_t is the body mass of juvenile

oozoids and Bp_t is the body mass of post-release oozoids at time t.

Thalia democratica body mass (mg C m^{-3}) was calculated based on length (Deibel, 1985):

$$Bf_t = o(Lf_t)^p \quad (17)$$

where o and p are constants. The same equation is used for the other stages.

Reproduction

Female reproduction results in only one oozoid offspring per parent (Heron, 1972) and is calculated:

$$Rf_t = Rmax_t \times Rmf_t \quad (18)$$

where Rf_t is the average female reproduction rate (oozoids $female^{-1}$), $Rmax_t$ is the maximum average female reproduction rate (oozoids $female^{-1}$) and Rmf_t is the proportional reproduction success related to male density at time t.

As the size range of reproductive females varies (from 4 to 10 mm), a logistic curve was used to represent cumulative size-dependent female reproduction. It assumes that 50% of females will be reproducing at 8 mm (Heron, 1972), and as they increase in size the likelihood of reproducing increases to a maximum average of one offspring per female. Therefore, maximum female reproduction is:

$$Rmax_t = \frac{1}{1 + e^{-(Lf_t - L_{50})}} \quad (19)$$

where the numerator is the maximum reproduction rate per individual female (1 oozoid $female^{-1}$) and L_{50} (mm) is the length at which 50% of the female population has reproduced.

As male fertilization is necessary for the production of oozoids, actual reproduction rate will be dependent on the abundance of males. To incorporate male abundance into female reproduction rate we used:

$$Rmf_t = \frac{MF_t}{MF_{50} + MF_t} \quad (20)$$

where MF_t is the male-to-female ratio at time t and MF_{50} is the ratio of males-to-females that gives 50% reproduction efficiency.

For oozoid reproduction, it was assumed that all chains of female buds will be released when an individual reached 10 mm (average size for female bud release; Heron, 1972). For each generation, the number of offspring released per oozoid was selected from a normal distribution:

$$Rj_t \sim \mathcal{N}(\mu_{Rj}, \sigma_{Rj}) \quad (21)$$

where Rj_t is the oozoid reproduction rate (females $oozoid^{-1}$) at time t and μ_{Rj} and σ_{Rj} are the mean and standard deviation of the female offspring released per oozoid.

Model simulation

To compare model outputs with observed salp data, and to evaluate predicted seasonal and yearly variation in salp abundance, simulations were run for a 10-year period (2003–2012). Three locations were chosen along the New South Wales coast: Coffs Harbour (30.29°S, 153.16°E), Sydney (34°S, 151.15°E) and Eden (37.08°S, 149.96°E). The Coffs Harbour region is subtropical and dominated by the East Australian Current (EAC; Suthers *et al.*, 2011). Both the Sydney and Eden regions are temperate and south of the EAC separation zone (Suthers *et al.*, 2011). Daily observations of SST and chl-*a* data were obtained from the Moderate Resolution Imaging Spectroradiometer Aqua Satellite (MODIS) via the Integrated Marine Observing System (IMOS) Data Portal (http://imos.aodn.org.au/imos/) at 1-km resolution. To maximize data availability, 7-day running averages were calculated for both SST and chl-*a* concentration before data were interpolated into hourly increments to match the time step of the numerical model. SST and chl-*a* data were averaged seasonally, and compared across years with a two-way analysis of variance (ANOVA). Tukey's HSD test was used for a posteriori pair-wise comparisons between factor levels for all ANOVAs.

For each location, the time-series simulation was spun-up for 10 years to allow the model to reach a quasi steady-state before commencing the model simulations. The initial abundances of females and males to begin a simulation were derived from Henschke *et al.* (Henschke *et al.*, 2014). The initial abundances of juvenile oozoids and post-release oozoids were set at zero in order to only have one reproductive generation existing at a time. Following the spin-up, the model state from the final time step was used to initialize the 10-year model simulation. Model outputs were averaged monthly and seasonally to correspond with observational data. Zooplankton have been sampled near monthly at the Port Hacking National Reference Station (near Sydney) from 2002, and salp abundances were used to validate the Sydney model simulation. For a full description of the sampling method, see Henschke *et al.* (Henschke *et al.*, 2014). Port

Hacking zooplankton data are freely available via the Integrated Marine Observing System (IMOS) data portal. (http://imos.aodn.org.au/.)

Sensitivity analysis

A sensitivity analysis was conducted on the model simulation as per Smith *et al.* (Smith *et al.*, 2012). This involved randomly varying a selection of input parameters over many iterations, followed by a model selection to discern which input variables were most influential to selected model outputs. Most parameters were included in the analysis, especially those with input values that were uncertain (e.g. the maximum growth coefficient, h), or if they were likely to vary biologically (e.g. temperature, T_t). Random sets of parameter values were created at either the assigned value or $\pm 10\%$ of the value. The model output variables that were tracked for the sensitivity analysis were population abundance, population biomass, stage-specific salp abundance, blastozooid-to-oozoid ratio and generation time. For this analysis, the population model was run at sub-optimal temperatures ($T =$ 14°C) to better identify the sensitivity of model outputs to temperature. To test the sensitivity of the model outputs to phytoplankton concentration, the model was run at a constant phytoplankton concentration (0.39 mg C m^{-3}; average of Sydney time-series). Random parameter values were varied across each simulation until the variance for the average model outputs stabilized (1000 variations of random parameters). Parameter values were standardized according to Kleijnen (Kleijnen, 1997); and bidirectional step-wise regression analysis and Akaike's Information Criteria were used to determine the most influential input variables for each model output.

RESULTS

Lefkovitch matrix model

Based on the Lefkovitch matrix the *T. democratica* population stabilizes and grows at a rate (λ) of 1.32 day^{-1}. The proportional sensitivity (or elasticity) of λ to changes in F_i, P_i and G_i is given in Fig. 3. As the elasticity values in the elasticity matrix sum to one (Caswell, 1989), they show the relative contribution of each matrix element to λ and can be plotted. When conditions are kept stable (i.e. optimal temperature and food resulting in maximum growth and reproduction rates), juvenile oozoids appear to be the most important generation promoting population growth, with a 1% increase in the probability of juvenile oozoid survival (P_i) resulting in a 0.29% increase in population growth (Fig. 3).

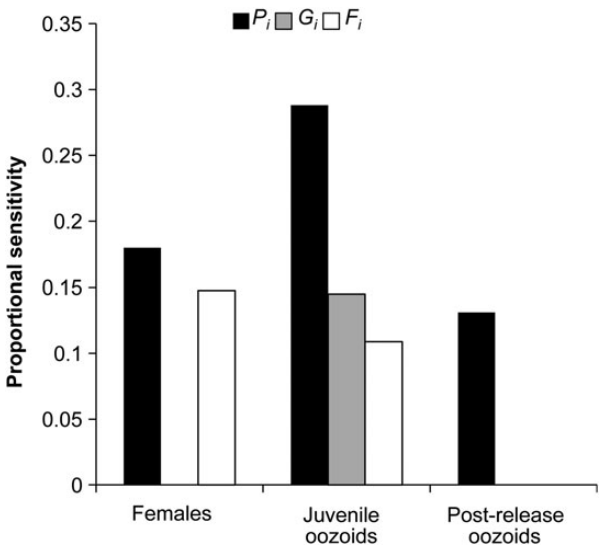

Fig. 3. The elasticity, or proportional sensitivity of population growth (λ) to changes in survival within the same stage (black bars), survival while transitioning to the next stage (grey bars) or fecundity (white bars). Because the elasticities of these matrix elements sum to 1, they can be compared directly in terms of their contribution to the population growth rate. Males are not included in the graph as λ was not sensitive to variation in male survival. P_i is the probability of surviving and remaining in the same stage, G_i is the probability of surviving and growing to the next ith stage and F_i is the stage-specific fecundity.

Time-series simulation

Strong seasonal trends were observed in SST and chl-*a* concentration across all locations (Fig. 4). SST was significantly higher in Coffs Harbour compared with Sydney and was lowest overall in Eden ($F_{2,108} = 659.17$, $P < 0.001$). Across all locations, SST was higher in summer and autumn ($F_{3,108} = 423.75$, $P < 0.001$; Table IV). Warmer SST was associated with lower chl-*a* concentration, with the highest chl-*a* concentration occurring in winter and spring ($F_{3,108} = 66.96$, $P < 0.001$; Table IV), and the highest overall chl-*a* concentration in Eden ($F_{2,108} = 65.77$, $P < 0.001$).

Mean salp abundance across the 10 years ranged from 74 to 419 ind m^{-3} at Sydney (overall mean $\pm$ SD; 205 $\pm$ 33) and 181 to 661 ind. m^{-3} at Eden (352 $\pm$ 57; Fig. 5). Seasonal abundances also varied across locations (Fig. 5; Table IV). Salp abundances were higher during winter (77 ind. m^{-3}) and spring (124 ind. m^{-3}) at Sydney compared with summer and autumn (2 and 2 ind. m^{-3}, respectively). Spring and winter also corresponded to shorter generation times (8 and 7 days respectively) at Sydney compared with 17 days in both summer and autumn. Model-simulated values for Sydney correspond well to monthly trends seen in *T. democratica* abundances at the Port Hacking National Reference Station, particularly during winter and spring (June–November; Port Hacking mean = 45.81 $\pm$

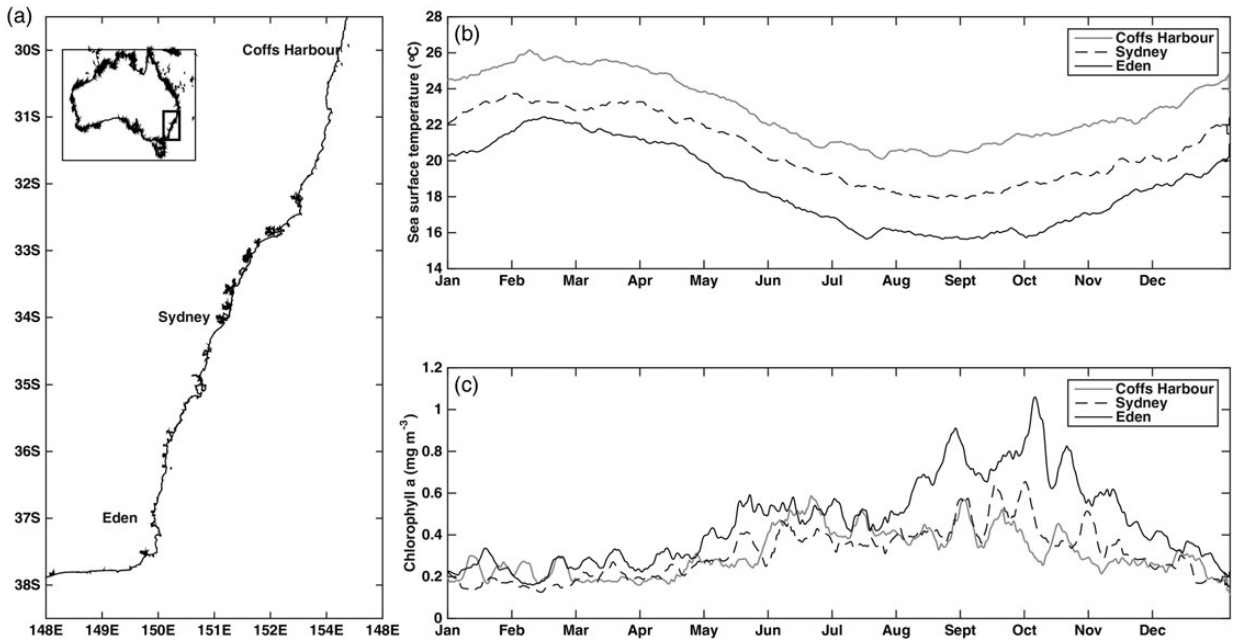

Fig. 4. (**a**) Location map showing areas along the New South Wales coast that were input in the time-series simulation. The locations are Coffs Harbour (grey), Sydney (dashed), and Eden (black). Long-term (2003–2012) averaged satellite-derived sea surface temperature (**b**) and chlorophyll *a* biomass (**c**) showed some variation across locations, and seasonality in oceanographic conditions.

Table IV: Results of the long-term (2003–2012) seasonal analysis at Coffs Harbour, Sydney and Eden

Location	Season	Sea surface temperature (°C)	Chlorophyll *a* (mg m^{-3})	*T. democratica* abundance (ind. m^{-3})	Generation time (days)	B-O ratio	Proportional abundance (%)			
							F	M	J	PR
Coffs Harbour	Summer	24.33 ± 0.50	0.23 ± 0.03	–	–	–	–	–	–	–
	Autumn	24.33 ± 0.50	0.23 ± 0.03	–	–	–	–	–	–	–
	Winter	20.78 ± 0.37	0.44 ± 0.09	–	–	–	–	–	–	–
	Spring	21.75 ± 0.49	0.33 ± 0.09	–	–	–	–	–	–	–
Sydney	Summer	22.26 ± 0.58	0.25 ± 0.06	1.67 ± 5.21	17.35 ± 3.24	5.01	76	4	19	1
	Autumn	22.26 ± 0.58	0.25 ± 0.06	1.67 ± 5.21	17.35 ± 3.24	5.01	76	4	19	1
	Winter	18.70 ± 0.62	0.40 ± 0.09	76.69 ± 72.44	7.19 ± 0.66	11.80	88	4	8	1
	Spring	19.13 ± 0.47	0.40 ± 0.08	124.44 ± 120.69	7.70 ± 0.68	10.47	73	16	10	1
Eden	Summer	20.41 ± 0.52	0.35 ± 0.05	65.73 ± 87.21	9.80 ± 1.13	9.11	84	4	11	1
	Autumn	20.41 ± 0.52	0.35 ± 0.05	65.73 ± 87.21	9.80 ± 1.13	9.11	84	4	11	1
	Winter	16.40 ± 0.69	0.57 ± 0.07	138.46 ± 83.35	6.59 ± 0.32	11.27	86	4	9	1
	Spring	16.89 ± 0.38	0.65 ± 0.12	81.69 ± 83.90	6.55 ± 0.16	10.64	84	5	10	1

Values are means (± SD).
B-O ratio, blastozooid-to-oozoid ratio; F, females; M, males; J, juvenile oozoids; PR, post-release oozoids.

140.40, $n = 93$; Fig. 6). At Eden, salp abundances were higher in winter (138 ind. m^{-3}) compared with all other seasons (66–82 ind. m^{-3}). Generation times at Eden ranged from 7 days (winter and spring) to 10 days (summer and autumn). Females were the most dominant life history stage across each location (~81%; Table IV), with juvenile oozoids the second most dominant life history stage (~12%). The blastozooid-to-oozoid ratio ranged from 5 to 11 at Sydney, and 9 to 11 at Eden (Table IV). After the initial spin up, no salps survived at Coffs Harbour, so no further results are presented here.

Sensitivity analysis

Given that the influence of temperature (T_t) within this model is proportional to ΔT, when ΔT approaches zero (i.e. $T_t = T_{opt}$), the sensitivity of each model output to temperature approaches zero. During sub-optimal temperature conditions (i.e. $\Delta T > 0$), the most parsimonious model explaining the variation of *T. democratica* population abundance consisted of eight parameters ($R^2 = 0.31$, $F = 56.4$, $P < 0.001$; Fig. 7*a*). Temperature (T), the growth rate coefficient (h), the female mortality coefficient

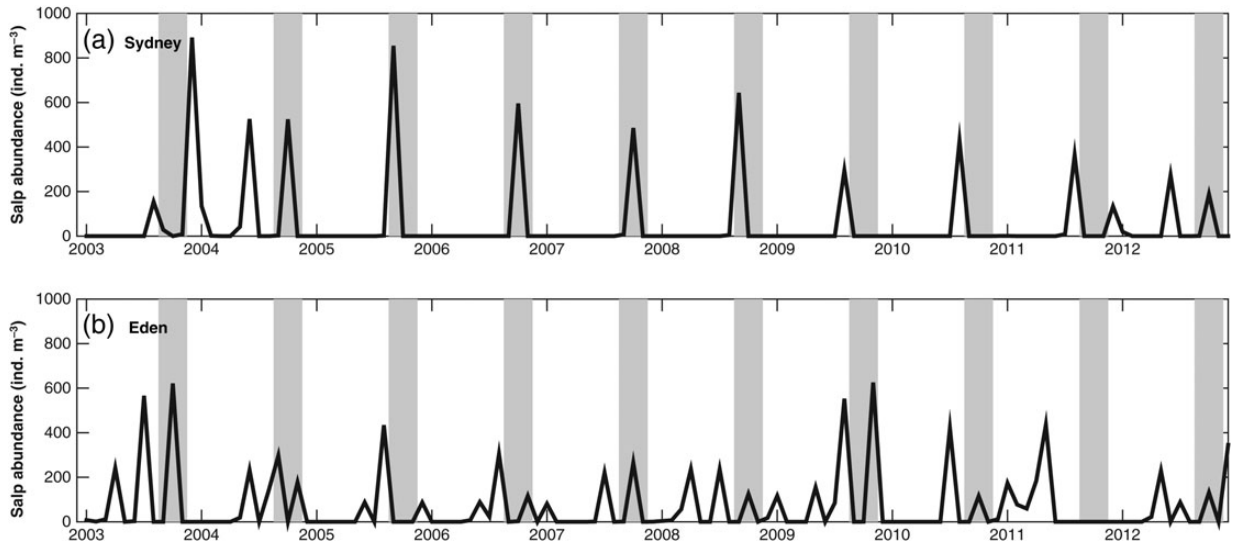

Fig. 5. Time-series model simulation showing ten years of simulated *Thalia democratica* abundances (2003–2012) at (**a**) Sydney and (**b**) Eden. Coffs Harbour values are not represented as the simulation showed zero salp survival at Coffs Harbour. Shaded bars represent spring (September–November).

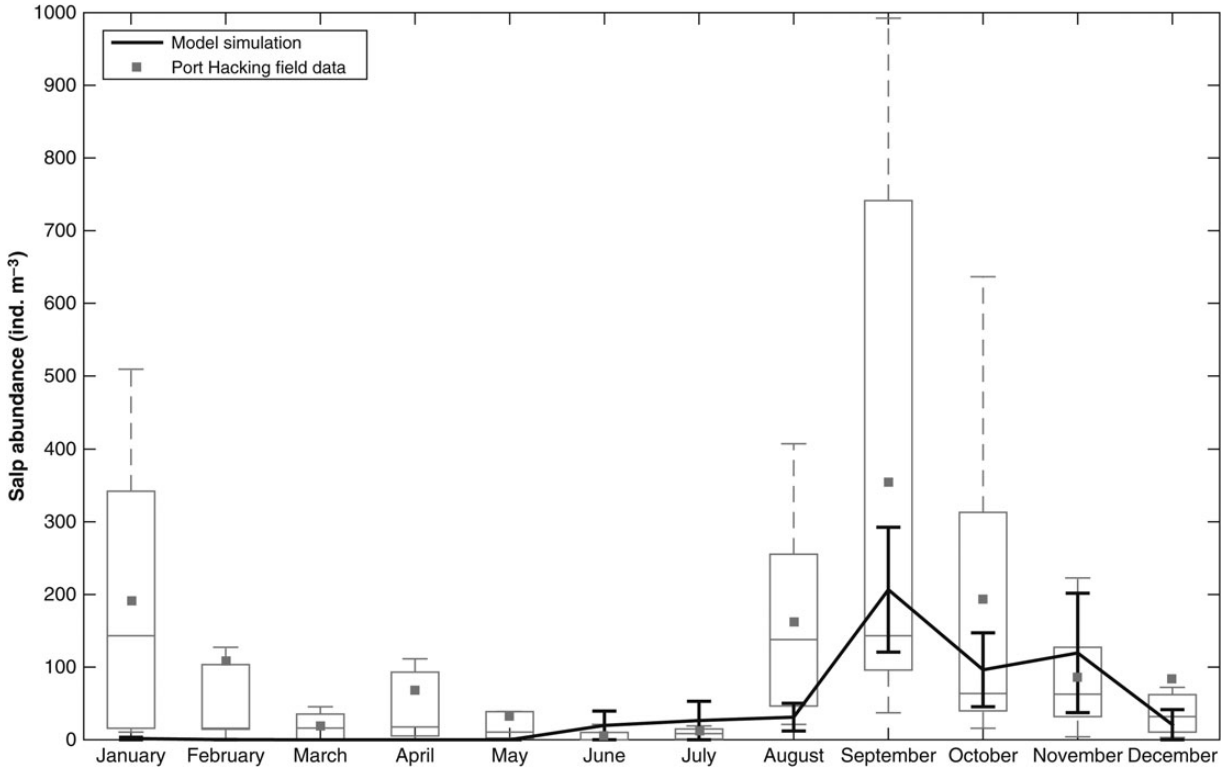

Fig. 6. Box and whisker plot of *Thalia democratica* abundance sampled at Port Hacking, Sydney (2003–2010). Means are represented by grey squares. Black line represents the mean (± SE) monthly *T. democratica* abundances simulated from the time-series model at Sydney (2003–2010).

(*a*) and the length at which 50% of females were reproducing (L_{50}) had the largest influences on total salp abundance. The best model for generation time contained four parameters, and explained 95% of the variation ($F = 4289$, $P < 0.001$; Fig. 7*b*). $\mathcal{T}$ and h were the parameters with the largest influence on generation time. $\mathcal{T}$ and L_{50} had by far the largest influence on the blastozooid-to-oozoid ratio ($R^2 = 0.72$, $F = 254.5$, $P < 0.001$; Fig. 7*c*). $\mathcal{T}$, h, a and L_{50} played the largest influences on female ($R^2 = 0.30$, $F = 54.3$, $P < 0.001$; Fig. 7*d*),

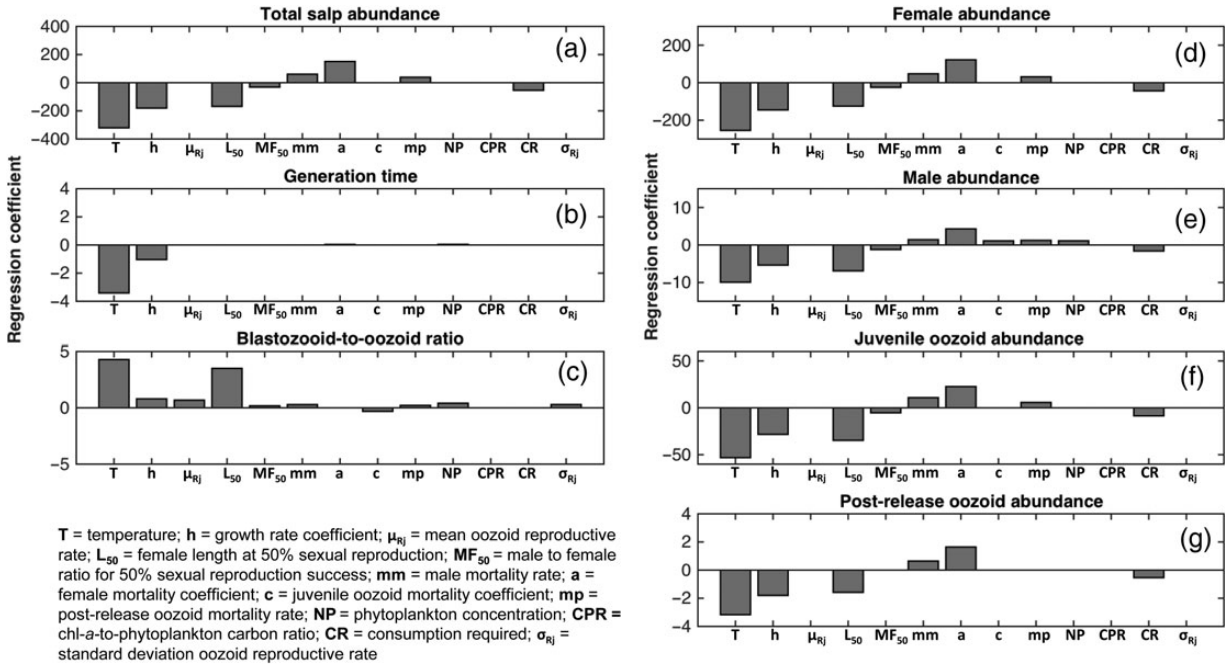

Fig. 7. Results of sensitivity analysis for a sub-optimal temperature run (14°C). The bars represent the significant coefficients of model parameters signifying their influence on (**a**) total salp abundance, (**b**) generation time, (**c**) blastozooid-to-oozoid ratio, (**d**) female abundance, (**e**) male abundance, (**f**) juvenile oozoid abundance and (**g**) post-release oozoid abundance.

male ($R^2 = 0.33$, $F = 48.27$, $P < 0.001$; Fig. 7*e*), juvenile oozoid ($R^2 = 0.33$, $F = 62.16$, $P < 0.001$; Fig. 7*f*) and post-release oozoid abundances ($R^2 = 0.31$, $F = 73.66$, $P < 0.001$; Fig. 7g).

DISCUSSION

Our size-structured population model is the first *T. democratica* population model to incorporate food-based density dependence, and shows that SST and phytoplankton abundance (chl-*a*) can be sufficient drivers to create realistic large-scale population dynamics of *T. democratica*. Juvenile oozoids were identified as the life history stage most influential to population biomass by both the Lefkovitch matrix and the size-structured population model. This model demonstrates that population-level traits need to be considered when seeking to understand the location and biomass of salp swarms.

Comparison of the modelled salp population with field estimates

The salp abundance estimated from our size-structured population model agreed well with broad-scale field observations. The modelled mean spring population abundances of *T. democratica* (82 and 124 ind. m^{-3}) were reasonably similar to mean spring abundances observed at Port Hacking from 2002 to 2010 (144 ind. m^{-3}) and in the Tasman Sea from 2008 to 2010 (92–1312 ind. m^{-3}; Henschke *et al.*, 2014). These abundances are generally dominated by blastozooids (~90% of the total population; Henschke *et al.*, 2011) which result in blastozooid-to-oozoid ratios ranging from 8.8 to 11.2 (Henschke *et al.*, 2014). Proportional abundances of blastozooids (80–90%) and oozoids (9–20%) and the mean blastozooid-to-oozoid ratio (9) estimated in the simulation were consistent with these field studies. The large variation observed in the modelled proportional abundances of oozoids could be explained by the patchiness of salp swarms, and the undersampling of oozoids in the field due to their low abundances (Hamner *et al.*, 1975).

Average generation times (7–17 days) were within the range previously observed (2–21 days; Braconnot, 1963; Heron, 1972; Deibel, 1982; Tsuda and Nemoto, 1992). Generation time is negatively correlated with growth rates, and the maximum growth rate used in this model [Equation (15)] equates to a generation time of 2 days (Heron, 1972). Everett *et al.* (Everett *et al.*, 2011) demonstrated that it would be unsustainable for a salp swarm in the Tasman Sea to be growing as fast as suggested by Heron (Heron, 1972) as they would deplete all the nitrogen supporting phytoplankton within the water column in less than a day. The generation time achieved in this model under optimum conditions such as in spring was 7–8 days, which is a more realistic value and corresponds

well to the shortest duration of an *in situ* salp swarm (1 week; Deibel and Paffenhofer, 2009). The agreement between simulated salp abundances and generation times and their field estimates suggests that the parameterization between maximum growth rate and environmental conditions (SST and phytoplankton concentration) used in this model was appropriate.

Pattern of long-term and seasonal salp abundance

The seasonal variation of salps sampled at Port Hacking was well captured by the model simulation; however, the simulation underestimated salp abundances occurring during late summer and autumn (February–May; Fig. 6), suggesting that other factors could be promoting summer swarms of salps in the field. It would be ideal to use other long-term datasets to aid validation of our model, but there is a lack of spatially resolved zooplankton studies within the Tasman Sea. Apart from the Port Hacking study (2002–2010; Henschke *et al.*, 2014), the most comprehensive studies sampling salps occurred from 1938 to 1941 (Thompson and Kesteven, 1942) and from 1957 to 1960 (Tranter, 1962). In these early studies, mean yearly salp abundances along the south-east coast of Australia (south from Sydney) did not differ significantly with latitude (Tranter, 1962) which agrees with the output of the time-series simulation in the current study for Sydney and Eden.

The absence of salp survival at Coffs Harbour suggests that this location has poor conditions for the formation of salp swarms, probably due to the high SST experienced (mean = 24.3°C). Historical samples found very low abundances of *T. democratica* at or north of Coffs Harbour and a total absence of salp swarms (Thompson and Kesteven, 1942; Tranter, 1962). This is consistent with monthly zooplankton sampling (from 2009) north of Coffs Harbour near Stradbroke Island (27°S), that has found *T. democratica* occurs in low abundances year round (<10 salps m^{-3}; IMOS, 2014).

The time-series simulation showed strong seasonal variation at Sydney, with *T. democratica* abundances significantly higher during winter and spring. Winter and spring were associated with lower SST and higher chl-*a* concentration (Table IV), which suggests that higher salp abundances at Sydney are associated with oceanographic conditions that promote phytoplankton blooms. Seasonal variation in *T. democratica* abundance is well documented off Sydney and Eden, with abundances generally being higher in spring off Sydney (Thompson and Kesteven, 1942; Tranter, 1962; Baird *et al.*, 2011; Henschke *et al.*, 2014) and higher in late spring and summer off Eden (Thompson and Kesteven, 1942; Tranter, 1962; Baird *et al.*, 2011).

Compared to Sydney, the range in seasonal abundances of salps was not as strong at Eden. Simulated salp abundances were consistently high throughout the year at Eden which could be a result of SST being near optimum year round (mean = 18.6°C). The cooler waters at Eden would favour salps, compared with warmer waters further north (Baird *et al.*, 2011). Compared with other locations along the south-east Australian coast, Eden also has a strong seasonal chl-*a* signal, with higher chl-*a* concentration observed in winter and spring (Everett *et al.*, 2014). Generally, simulated salp abundances were higher in winter and spring, which is likely to be promoted by the higher chl-*a* (phytoplankton) concentrations in these seasons.

Sensitivity analysis

The sensitivity analysis identified that salp generation time was most sensitive to changes in water temperature and maximum growth rate. This indicates that generation time decreases (i.e. salp growth rate increases) with temperature towards the optimum due to the proportional relationship between temperature and growth. This relationship would reverse as temperatures increase above the optimum. Total salp abundance and abundances of each life history stage were most sensitive to changes in temperature (T), the growth rate coefficient (h), the female mortality coefficient (a) and the length at which 50% of females were reproducing (L_{50}). Abundance was negatively related to T, h and L_{50} and positively related to a. Reducing the size at which females reproduce and increasing female mortality would result in an overall decrease in the proportion of females (due to mortality and some becoming males earlier), and an increase in the proportion of oozoids. A negative relationship between temperature and the growth coefficient also indicates that higher salp abundances occur as growth rate is reduced. Reducing the growth rate would result in a delay before the next generation of females is born, as oozoids only give birth once they reach 10 mm. This suggests that higher salp abundances occur when juvenile oozoid survival is favoured over females. When conditions are kept stable, the survival of juvenile oozoids was found by the Lefkovitch matrix model to be the most influential life history parameter to a salp population. Salp populations with low abundances have been found with a paucity of oozoid stages (Henschke *et al.*, 2011; Loeb and Santora, 2012), confirming that oozoids are necessary to increase population abundances. This is most likely due to their high reproductive rates compared with females (up to 240 offspring per individual; Heron, 1972).

Model limitations

Numerous parameter values remain uncertain in this salp population model due to a lack of experimental data for *T. democratica*. Experimental data could improve the accuracy of model outputs, and the sensitivity analysis can be used to prioritize parameters for study. The model assumption most in need of empirical support is the length at which 50% of females were reproducing (L_{50}). Variations in L_{50} significantly influenced the abundances of each life history stage. The size at which 50% of females release oozoids is unknown, and the size range for reproductive females is large (4–10 mm; Heron, 1972). Understanding the conditions which may influence the length at which females release juvenile oozoids may be key to predicting salp swarm magnitude, particularly if juvenile oozoids are the most influential life history stage in a salp population.

Both temperature and phytoplankton concentration greatly influenced population dynamics and abundances. This was expected given that they were the only two environmental parameters used in the model. The influence of temperature was more pronounced, and this is echoed in the field (Lucas *et al.*, 2014; Stone and Steinberg, 2014). Long-term studies have found it difficult to correlate salp abundance directly to chl-*a*, most likely due to chl-*a* encompassing both growth and removal of carbon (Lucas *et al.*, 2014). Although both temperature and phytoplankton concentration (chl-*a*) are probably the main drivers of salp abundance (Licandro *et al.*, 2006; Deibel and Paffenhofer, 2009), incorporating other environmental parameters such as nutrients, and more complex model structures such as a dynamic chl-*a* model (i.e. a predator–prey analysis rather than a time-series analysis), may improve the model's accuracy.

Predicting *Thalia democratica* swarms

The lack of long-term zooplankton abundance data means that there is little understanding of how zooplankton populations respond to environmental variation, and there is significant uncertainty around the trajectory of salp biomass in a changing ocean (Brotz *et al.*, 2012; Condon *et al.*, 2013). The salp population model in this study enabled an analysis of the seasonal and broad spatial variation of *T. democratica* swarms. Salp population dynamics were driven by changes in temperature and phytoplankton concentration that generally occur during winter and spring, consistent with field observations. To increase the predictive capabilities of this model, future research should prioritize the relationships between salp growth and ingestion rates, and the conditions altering the size at which females reproduce. Running this model with different salp species and in different oceanographic areas will help to broaden the scope of these findings.

ACKNOWLEDGEMENTS

We would like to thank Mark Baird for insightful discussions throughout the course of this manuscript and the Plankton Ecology Laboratory, CSIRO, for Port Hacking zooplankton identifications. We acknowledge the valuable reviews that have helped to improve the clarity and focus of this manuscript. This is contribution 150 from the Sydney Institute of Marine Science.

FUNDING

This project was funded by the University of New South Wales and the Australian Research Council. Remotely sensed oceanographic data and salp abundance data were sourced from the Integrated Marine Observing System (IMOS) - IMOS is a national collaborative research infrastructure, supported by Australian Government.

REFERENCES

Andersen, V. and Nival, P. (1986) A model of the population-dynamics of salps in coastal waters of the Ligurian Sea. *J. Plankton Res.*, **8**, 1091–1110.

Baird, M. E., Everett, J. D. and Suthers, I. M. (2011) Analysis of south-east Australian zooplankton observations of 1938–42 using synoptic oceanographic conditions. *Deep Sea Res. Part II*, **58**, 699–711.

Blackburn, M. (1979) Thaliacea of the California Current region: relations to temperature, chlorophyll, currents, and upwelling. *California Cooperative Oceanic Fisheries Investigations Reports*, **20**, 184–193.

Braconnot, J. C. (1963) Study of the annual cycle of salps and doliolids in Rade de Villefranche-sur-mer. *ICES/CIEM Int. Counc. Explor. Sea*, **28**, 21–36.

Brotz, L., Cheung, W. W. L., Kleisner, K., Pakhomov, E. and Pauly, D. (2012) Increasing jellyfish populations: trends in Large Marine Ecosystems. *Hydrobiologia*, **690**, 3–20.

Bruland, K. W. and Silver, M. W. (1981) Sinking rates of fecal pellets from gelatinous zooplankton (Salps, Pteropods, Doliolids). *Mar. Biol.*, **63**, 295–300.

Caswell, H. (1989) *Matrix Population Modeling*. Sinauer Associates, Sunerland, Massachusetts, USA.

Christensen, V. and Pauly, D. (1992) ECOPATH II - a software for balancing steady-state ecosystem models and calculating network characteristics. *Ecol. Model.*, **61**, 169–185.

Condon, R. H., Duarte, C. M., Pitt, K. A., Robinson, K. L., Lucas, C. H., Sutherland, K. R., Mianzan, H., Bogeberg, M. *et al.* (2013) Recurrent jellyfish blooms are a consequence of global oscillations. *Proc. Natl. Acad. Sci. USA*, **110**, 1000–1005.

Deibel, D. (1982) Laboratory determined mortality, fecundity and growth-rates of *Thalia democratica* Forskal and *Dolioletta gegenbauri* Uljanin (Tunicata, Thaliacea). *J. Plankton Res.*, **4**, 143–153.

Deibel, D. (1985) Clearance rates of the salp *Thalia democratica* fed naturally occurring particles. *Mar. Biol.*, **86**, 47–54.

Deibel, D. and Paffenhofer, G. A. (2009) Predictability of patches of neritic salps and doliolids (Tunicata, Thaliacea). *J. Plankton Res.*, **31**, 1571–1579.

Everett, J. D., Baird, M. E., Roughan, M., Suthers, I. M. and Doblin, M. A. (2014) Relative impact of seasonal and oceanographic drivers on surface chlorophyll *a* along a Western Boundary Current. *Prog. Oceanogr.*, **120**, 340–351.

Everett, J. D., Baird, M. E. and Suthers, I. M. (2011) Three-dimensional structure of a swarm of the salp *Thalia democratica* within a cold-core eddy off southeast Australia. *J. Geophys. Res.*, **116**, C12046.

Fischer, G., Futterer, D., Gersonde, R., Honjo, S., Ostermann, D. and Wefer, G. (1988) Seasonal variability of particle flux in the Weddell Sea and its relation to ice cover. *Nature*, **335**, 426–428.

Hamner, W. M., Madin, L. P., Alldredge, A. L., Gilmer, R. W. and Hamner, P. P. (1975) Underwater observations of gelatinous zooplankton: sampling problems, feeding biology, and behavior. *Limnol. Oceanogr.*, **20**, 907–917.

Harbison, G. and Gilmer, R. (1976) The feeding rates of the pelagic tunicate *Pegea confederata* and two other salps. *Limnol. Oceanogr.*, **21**, 517–528.

Harbison, G. R., McAlister, V. L. and Gilmer, R. W. (1986) The response of the salp, *Pegea confoederata*, to high levels of particulate material: starvation in the midst of plenty. *Limnol. Oceanogr.*, **31**, 371–382.

Henschke, N., Bowden, D. A., Everett, J. D., Holmes, S. P., Kloser, R. J., Lee, R. W. and Suthers, I. M. (2013) Salp-falls in the Tasman Sea: a major food input to deep sea benthos. *Mar. Ecol. Prog Ser.*, **491**, 165–175.

Henschke, N., Everett, J. D., Baird, M. E., Taylor, M. D. and Suthers, I. M. (2011) Distribution of life history stages of the salp *Thalia democratica* in shelf waters during a spring bloom. *Mar. Ecol. Prog Ser.*, **430**, 49–62.

Henschke, N., Everett, J. D., Doblin, M. A., Pitt, K. A., Richardson, A. J. and Suthers, I. M. (2014) Demography and interannual variability of salp swarms (*Thalia democratica*). *Mar. Biol.*, **161**, 149–163.

Heron, A. C. (1972) Population ecology of a colonizing species—pelagic tunicate *Thalia democratica*. 1. Individual growth-rate and generation time. *Oecologia*, **10**, 269–293.

Hobday, A. J., Okey, T. A., Poloczanska, E. S., Kunz, T. J. and Richardson, A. J. (2006) *Impacts of Climate Change on Australian Marine Life*, Australian Greenhouse Office, Canberra, Australia.

IMOS (2014) National Reference Station zooplankton counts. http://imos.aodn.org.au/ (9 May 2014, last accessed date).

Kleijnen, J. P. C. (1997) Sensitivity analysis and related analyses: a review of some statistical techniques. *J. Stat. Comput. Simul.*, **57**, 111–142.

Lebrato, M., de Jesus Mendes, P., Steinberg, D. K., Cartes, J. E., Jones, B. M., Birsa, L. B., Benavides, R. and Oschlies, A. (2013) Jelly biomass sinking speed reveals a fast carbon export mechanism. *Limnol. Oceanogr.*, **58**, 1113–1122.

Lefkovitch, L. P. (1965) The study of population growth in organisms grouped by stages. *Biometrics*, **21**, 1–18.

Licandro, P., Ibanez, F. and Etienne, M. (2006) Long-term fluctuations (1974–1999) of the salps *Thalia democratica* and *Salpa fusiformis* in the northwestern Mediterranean Sea: relationships with hydroclimatic variability. *Limnol. Oceanogr.*, **51**, 1832–1848.

Loeb, V. J. and Santora, J. A. (2012) Populaton dynamics of *Salpa thompsoni* near the Antarctic Peninsula: growth rates and interannual variations in reproductive activity (1993–2009). *Prog Oceanogr.*, **96**, 93–107.

Lotka, A. J. (1925) *Elements of Mathematical Biology*. Dover Publishers, New York.

Lucas, C. H., Jones, D. O. B., Hollyhead, C. J., Condon, R. H., Duarte, C. M., Graham, W. M., Robinson, K. L., Pitt, K. A. *et al.* (2014) Gelatinous zooplankton biomass in the global oceans: geographic variation and environmental drivers. *Global Ecol. Biogeogr.*, **23**, 701–714.

Menard, F., Dallot, S., Thomas, G. and Braconnot, J. C. (1994) Temporal fluctuations of two Mediterranean salp populations from 1967 to 1990—analysis of the influence of environmental variables using a Markov-chain model. *Mar. Ecol. Prog. Ser.*, **104**, 139–152.

Miller, R. L. and Cosson, J. (1997) Timing of sperm shedding and release of aggregates in the salp *Thalia democratica* (Urochordata: Thaliacea). *Mar. Biol.*, **129**, 607–614.

Mullin, M. M. (1983) In situ measurement of filtering rates of the salp, *Thalia democratica*, on phytoplankton and bacteria. *J. Plankton Res.*, **5**, 279–288.

Ney, J. J. (1990) Trophic economics in fisheries: assessment of demand-supply relationships between predators and prey. *Rev. Aquat. Sci.*, **2**, 55–82.

Poloczanska, E. S., Babcock, R. C., Butler, A., Hobday, A. J., Hoegh-Guldberg, O., Kunz, T. J., Matear, R., Milton, D. A. *et al.* (2007) Climate change and Australian marine life. *Oceanogr. Mar. Biol. Annu. Rev.*, **45**, 407–478.

Raskoff, K. A., Sommer, F. A., Hamner, W. M. and Cross, K. M. (2003) Collection and culture techniques for gelatinous zooplankton. *Biol. Bull.*, **204**, 68–80.

Smith, J. A., Baumgartner, L. J., Suthers, I. M., Ives, M. C. and Taylor, M. D. (2012) Estimating the stocking potential of fish in impoundments by modelling supply and steady-state demand. *Freshwater Biol.*, **57**, 1482–1499.

Stone, J. P. and Steinberg, D. K. (2014) Long-term time-series study of salp population dynamics in the Sargasso Sea. *Mar. Ecol. Prog Ser.*, **510**, 111–127.

Sutherland, K. R., Madin, L. P. and Stocker, R. (2010) Filtration of submicrometer particles by pelagic tunicates. *Proc. Natl. Acad. Sci. USA*, **107**, 15129–15134.

Suthers, I. M., Young, J. W., Baird, M. E., Roughan, M., Everett, J. D., Brassington, G. B., Byrne, M., Oke, P. R. *et al.* (2011) The strengthening East Australian Current, its eddies and biological effects—an introduction and overview. *Deep Sea Res. Part II*, **58**, 538–546.

Thompson, H. (1948) *Pelagic Tunicates of Australia*. Commonwealth Council for Scientific and Industrial Research, Melbourne.

Thompson, H. and Kesteven, G. L. (1942) Pelagic tunicates in the plankton of south-eastern Australian waters, and their place in oceanographic studies. In *Bulletin*, Council for Scientific and Industrial Research, 153, pp. 151–156.

Threlkeld, S. T. (1976) Starvation and the size structure of zooplankton communities. *Freshwat. Biol.*, **6**, 489–496.

Tranter, D. J. (1962) Zooplankton abundance in Australasian waters. *Mar. Freshwat. Res.*, **13**, 106–142.

Tsuda, A. and Nemoto, T. (1992) Distribution and growth of salps in a Kuroshio warm-core ring during summer 1987. *Deep Sea Res. Part A*, **39**(Suppl 1), S219–S229.

Vargas, C. A. and Madin, L. P. (2004) Zooplankton feeding ecology: clearance and ingestion rates of the salps *Thalia democratica*, *Cyclosalpa affinis* and *Salpa cylindrica* on naturally occurring particles in the Mid-Atlantic Bight. *J. Plankton Res.*, **26**, 827–833.